ISSN: 2753-4146 (Online)
Type of the Paper (Article)

The comparison of photogrammetric and terrestrial laser scanning methods in the documentation of small cultural heritage object – case study

Joanna Giżyńska[1], Emilia Komorowska[2] and Michał Kowalczyk[3]

[1] Graduate of Warsaw University of Technology; joannagizynska96@gmail.com
[2] Graduate of Warsaw University of Technology; emilia.komorowska96@gmail.com
[3] Department of Photogrammetry, Remote Sensing and Spatial Information Systems, Faculty of Geodesy and Cartography, Warsaw University of Technology, pl. Politechniki 1, Warsaw 00-661, Poland; michal.kowalczyk@pw.edu.pl
Corresponding Author: michal.kowalczyk@pw.edu.pl, Tel.: +48-22-234-5764

Received date: 07/11/2022; Accepted date: 12/12/2022; Published date: 16/12/2022

Abstract: This investigation aims to present the potential and limitations of using the photogrammetric and terrestrial laser scanning methods to document small cultural heritage objects. The object is a water pumping station building located in the Museum of King John III's Palace at Wilanów. It is situated near Lake Wilanowskie; hence the access to one wall was considerably limited. Data were acquired by the Terrestrial Laser Scanner Z+F 5006h and full-frame camera Canon 5D Mark II with the focal length - 17, 24, 28, 35 mm. The close-range images were processed in the Agisoft Metashape program, and the Structure-from-Motion with MultiView Stereo approach was utilised for the dense point cloud generation. The extended quality assessment analysis was conducted in the *CloudCompare* program, and the comparison between point clouds and cross-sections derived from the dataset was compared. The result of performed investigation shows that the point cloud generated from photos taken with a lens with a focal length 35 mm is characterised by the highest accuracy.

Keywords: Laser Scanning, MVS, Photogrammetry, Pumping Station, SfM

1. Introduction

Today, one of the more rapidly growing branches of surveying is building inventory. It is a design process performed to reconstruct or revitalise a building. It involves the preparation of appropriate documentation showing the monument's appearance pictorially or descriptively, including floor plans and facades, cross-sections and photographs [1,2]. It is created utilising activities carried out on the object, which includes surveys and measurements of the building in question and analysis of their results [3–7]. The inventory results are used by specialists in the construction and architectural industry, as well as by conservators of monuments [8–10]. They are aimed at carrying out conservation work and protecting buildings from destruction.

This paper presents the example of an inventory based on close-range photogrammetric techniques that allowed for accurate 3D shape reconstruction and a comparison of the methods and equipment used to select the most accurate development.

DOI: 10.33687/jmtchp.001.01.0013

2. Materials and Methods

This investigation aimed to compare the possibility of using different close-range photogrammetric surveying techniques in investigating the complex hard-to-access cultural heritage object. For this purpose, the Authors decided to validate the point clouds obtained from a Z+F 5006h phase scanner and the result of dense image-matching based on images taken by the Canon 5D Mark II camera. To generate point clouds Z+F LaserControl, LupoScan, and Agisoft Metashape software and for comparative analyses, the CloudCompare program was used

2.1. Test site description

The investigated object was the pumping station building located on the grounds of the King John III Palace Museum in Wilanów situated in Warsaw, Poland (Fig. 1). It is located between the shore of Wilanów Lake and the 17th-century Baroque geometric garden and a 19th-century English landscape park.

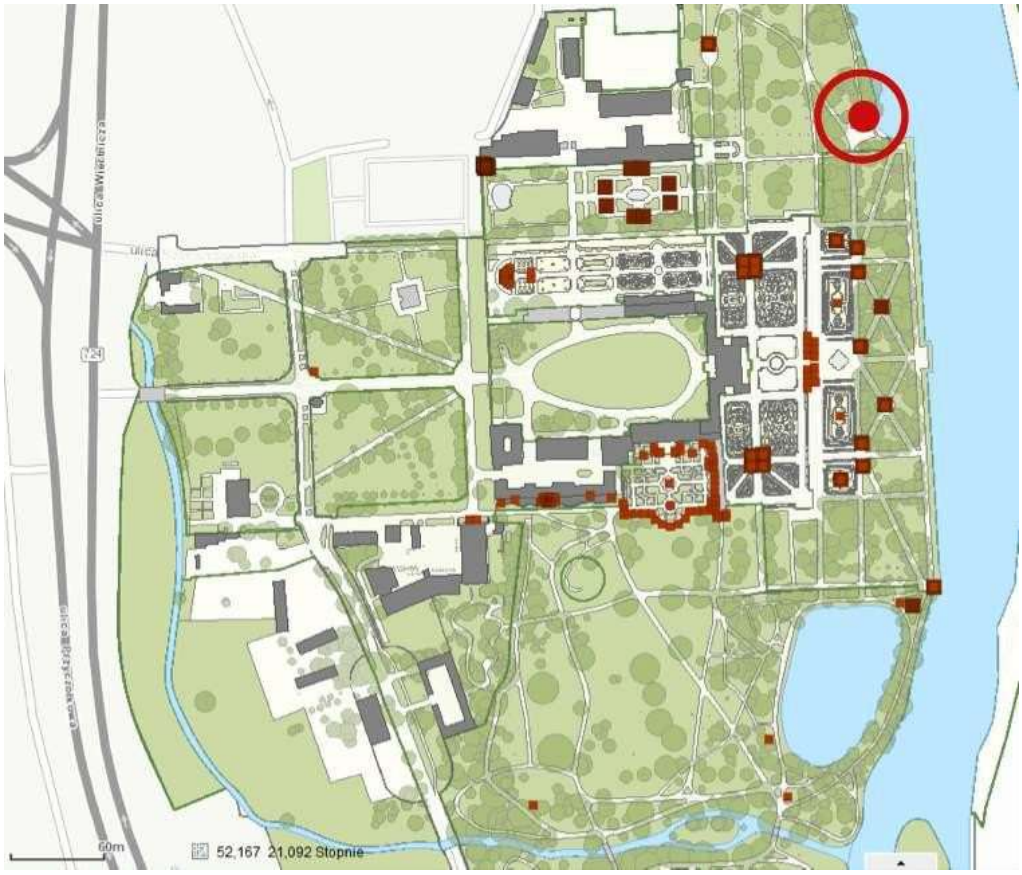

Figure 1. Location of the object on the grounds of the King John III Museum in Wilanow [11]

The pump house was designed by Henryk Marconi and was built in the middle of the XIX century. Its architecture is reminiscent of a medieval neo-Gothic castle (Fig. 2); it is one of the park's main attractions at the Wilanów Museum. In the past, the building was used to draw water from the lake via an underground water supply system to fountains located on the grounds of the Wilanów garden. It was a firefighting centre at one time, as it housed a fire truck inside. Currently, the pump house no longer performs these functions, is under conservation supervision and is only an educational space [12]. The building is located near a water reservoir. For this reason, access to the building is complicated, and its measured development requires thoughtful conducting fieldwork. Next to the pump house is a small marina for boats and gondolas, usually used by tourists visiting the Wilanów gardens.

DOI: 10.33687/jmtchp.001.01.0013

Figure 2. View of the pumping station from the side of Wilanow Lake (photo: W. Holnicki)

2.2. Methodology

2.2.1. Photogrammetric network design

The first stage of fieldwork was the determination of the photogrammetric network and placement of signalised control points in the form of black and white crosses in the format of A4 and A5(Fig. 3).

Figure 3. The example of signalised black-and-white control point [13]

Control points were distributed on the facade of the facility, on trees, and the tripods around the investigated object. It was important not to place too many control points on the building because too many of them would obscure the object too much. The points (format A5) numbered 2 - 5, 10, 11 and 18 were placed on the pumping station building, points (format A5) 1, 6 and 13 on tripods, and points 7 - 9, 12 and 14 - 17, in A4 format, on trees around the structure (Fig. 4). It was impossible to locate the control points on the facade of the building on the side of Wilanow Lake since the building is located near the adjacent to the water. During the measurements, a significant difficulty was the strong wind, which broke the points. For this reason, when compiling the results, it was impossible to use all the points deployed at the beginning of the work. Moved were points numbered 7 and 16, which were placed on trees around the pumping station.

DOI: 10.33687/jmtchp.001.01.0013

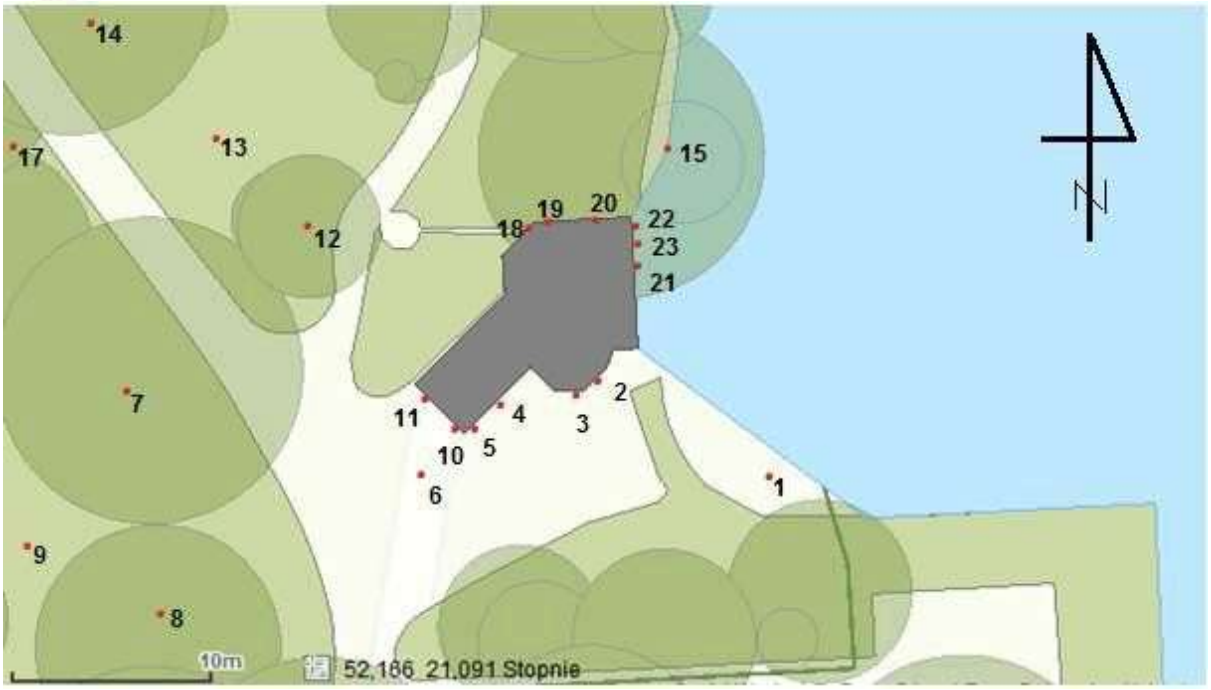

Figure 4. Control points distributions on the plan

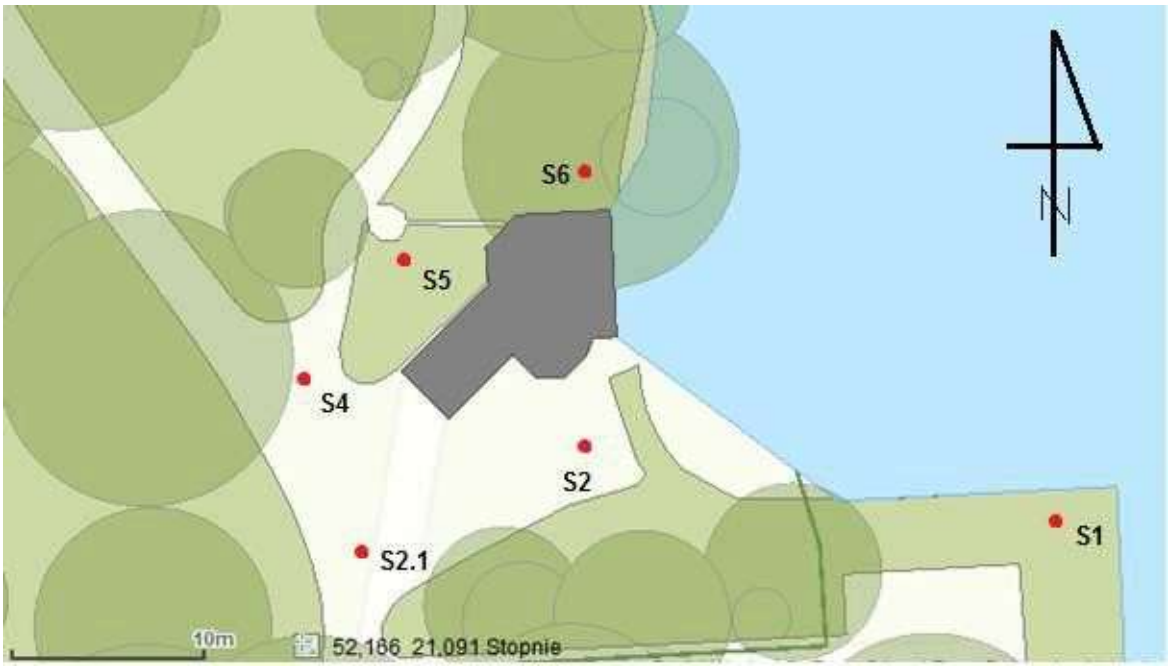

Figure 5. Terrestrial Laser Scanning positions

Once the signalled control points were distributed, selecting appropriate locations of the terrestrial laser scanner positions was necessary to reduce the measurement's labour intensity and accurately measure the object. It was also required to check whether the proper distance was maintained from the measured object (not exceeding 79 m). The object's location next to the lake was a significant difficulty in data acquisition. It was impossible to obtain data from the waterside facade from the other shore, as the distance between the wall of the pumping station and the distant shore exceeded 80 meters, with a scanner range of 75 meters. One of the positions had to be located on the peninsula next to the building so that the scanning range also covered part of the facility from the waterside and the distance of 79 meters was not exceeded. For our site, a total of six survey stations

were, in a way that allowed the connection of adjacent scans (Fig. 5). From scans located next to each other, at least 2 signalled points, and to increase accuracy - 3 or more.

2.2.2. The scheme of investigation

The preliminary work plan, the in-field work and the data processing were presented on a flowchart (Fig. 6). The blue font indicates the computer software used to develop a given stage of investigations.

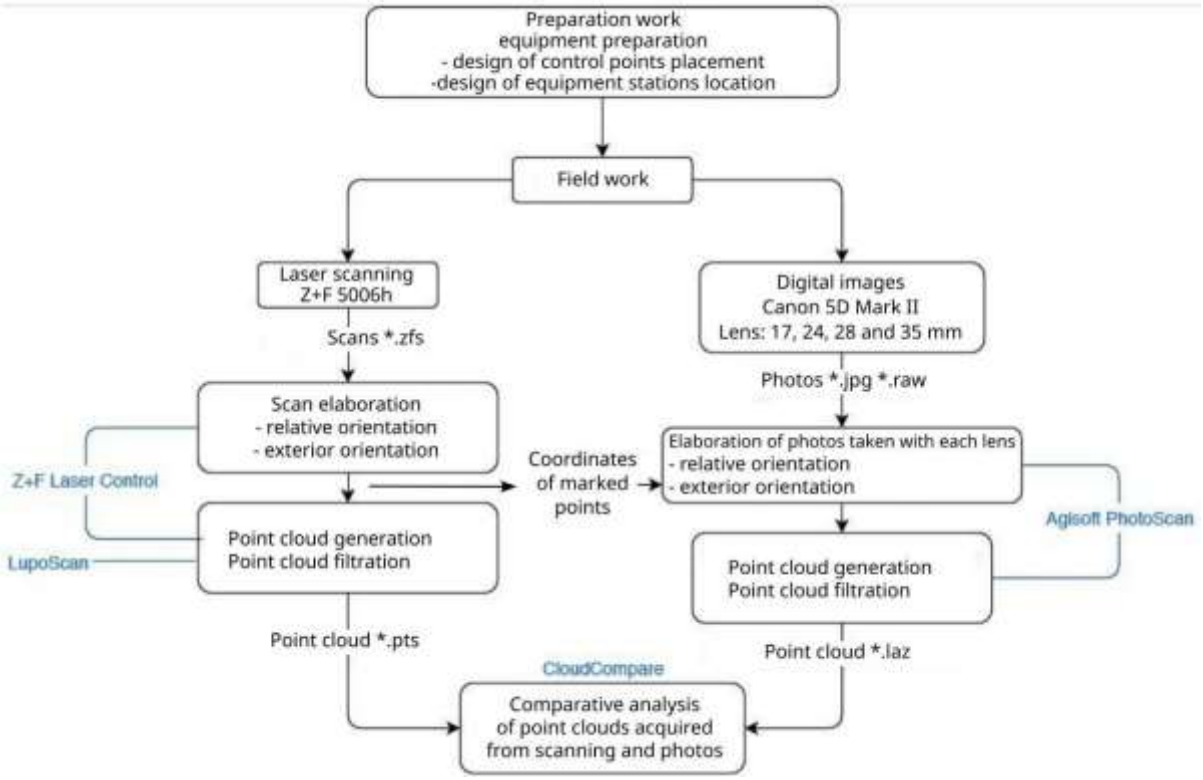

Figure 6. The block diagram of the work

The diagram shows the methodology of the performed experiment and investigation. The fieldwork was conducted jointly for image acquisition and performing terrestrial laser scanning. Due to that fact, it was necessary to plan and distribute control points (used in further stages as a reference for data orientation) together with the potential scanner and camera positions. The images acquisition part needed to take place in the shortest possible time, so there was no significant shifting of shadows on the object.

Cameral work included processing the scans and photos separately. The coordinates of the photogrammetric control point network were extracted from the scan orientation results and were used to fit the model derived from the photos into an assumed coordinate system.

The development of the scanning consisted of the following steps:

- observation of tie points, including signal control points, at least three to co-register each pair of scans - in Z+F LaserControl software
- register all scans into the assumed coordinate system using a 1:1 conformal transformation - Z+F LaserControl
- export control points coordinates used in the image processing step - Z+F LaserControl
- extraction points that represent the pumping station - LupoScan

- object point cloud filtering (geometrical filtration used for outliers removal) - LupoScan software (distances < 0.05 m; Intensity 1÷ 99%).

The processing of the images consisted of the following steps, separately for each group of images taken by the different lenses used for 3D shape reconstruction (Agisoft MetaShape program):

- division of the object into fragments
- preliminary adjustment of images using the SfM [14,15] method to improve the detection of control points
- assign the 3D coordinates of control points based on the results from the TLS data processing approach
- final images bundle adjustment with the self-calibration, using the SfM method
- combining fragments of the object into the defined coordinate system
- generate a dense point cloud using the MVS [16] method
- point cloud geometrical for outliers removal (separated parts removal)

The result of processing the scans and images were filtered point clouds in an assumed coordinate system. These included the scans and the object recorded with a camera equipped with a lens with focal lengths of 17, 24, 28, 35 mm, respectively.

This provided preparation for comparative analysis. The object of the study was to compare the set of points derived from the photos against the one derived from the laser scanning [17,18].

3. Results

3.1. Processing of terrestrial laser scanning data

The first step of terrestrial laser scanning point cloud processing was based on geometrical and radiometric filtration. The geometrical filtration assumed that the acceptable distance from neighbouring points should be less or equal to 0.05 m; if not, this point was treated as an outlier. In addition, points that were outside the range of the accepted reflection intensity (1 ÷ 99%) were also removed.

The most crucial step in TLS data processing was to measure the control points and additional tie points using Z+F LaserControl software (Fig. 7). The scans' positions were aligned into one selected scan position treated as a reference, using a conformal transformation that kept the transformation scale constant and equal 1.

The average deviation for the studied set of registrations was ± 3.3 mm, which is an acceptable result, given the density of points registered on the object's surface.

Figure 7. The example of a scan with the measured control points

3.2. Processing data from images

The first step in image processing was the relative orientation with the camera self-calibration in Agisoft Metashape software. The results of camera self-calibration for lenses with different focal lengths are shown in Table 1, and Figure 8 shows the image distribution diagrams for each lens.

Table 1. The results of camera self-calibration for each type of lens

	17 mm	24 mm	28 mm	35 mm
f [pix]	2744,79	3808,57	4441,13	5218,47
cx [pix]	7,38	-25,05	7,73	0,41
cy [pix]	2,36	-1,29	27,36	15,89
K1	-0,07242	-0,1057	-0,1114	-0,0508
K2	0,0480	0,1030	0,1371	0,0609
K3	-0,0114	-0,0094	-0,0344	-0,0139
P1	0,000113	-0,000164	-0,000739	0,000218
P2	0,000388	-0,000131	0,000048	0,000581

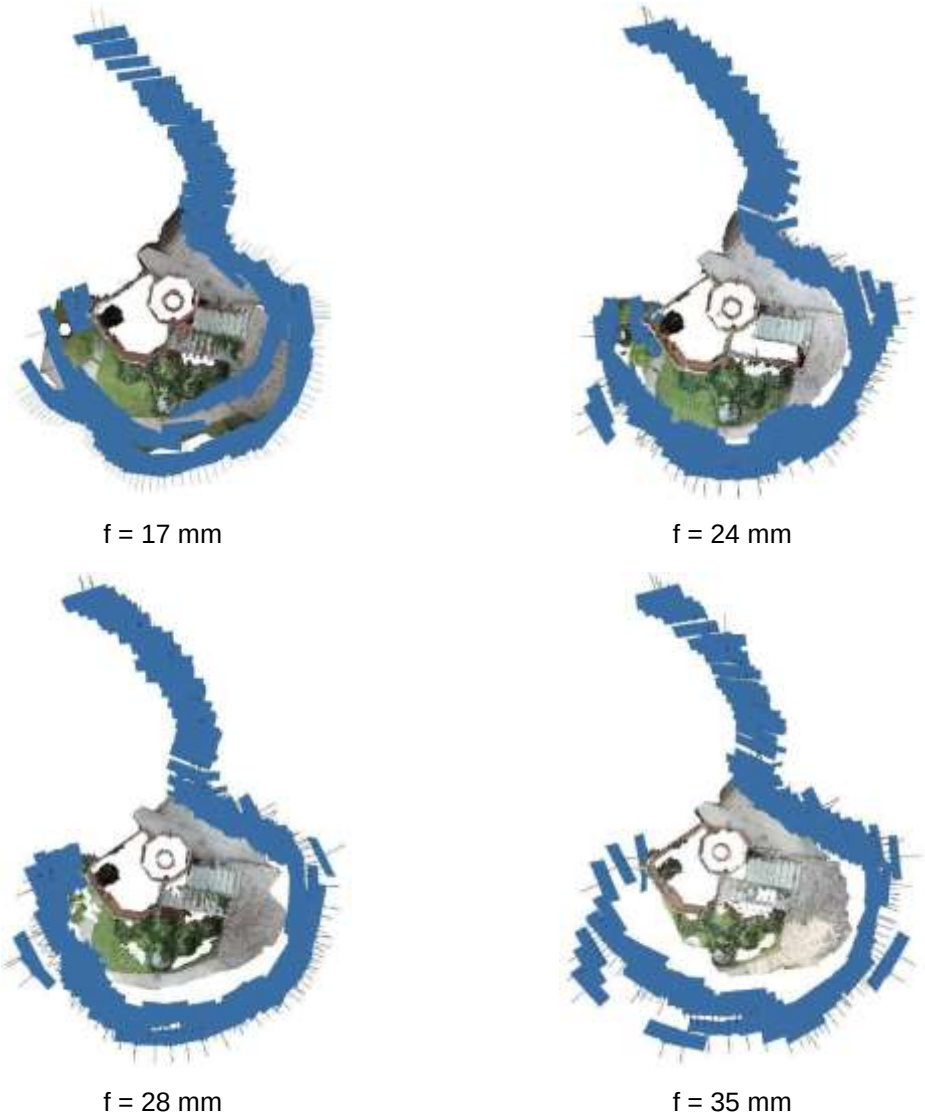

Figure 8. Image distribution diagrams for each lens

A preliminary visual assessment of the point clouds undertaken indicates that the best accuracy demonstrates a model made from images obtained from a lens with a focal length of 35 mm (Fig. 9). Further verification will be undertaken in the next stage - during the surface analysis of the point clouds.

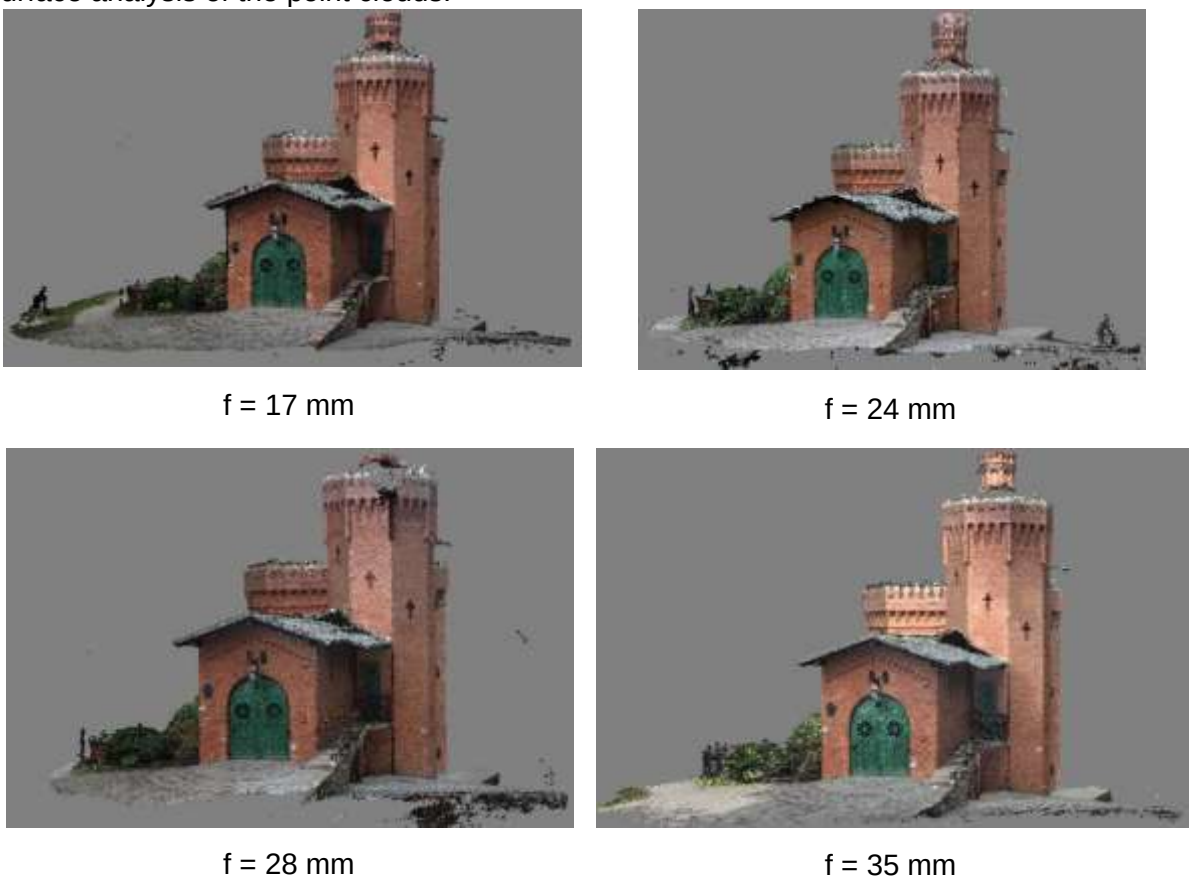

Figure 9. Point cloud, after filtering, generated from images taken using a lens with a focal length of 17, 24, 28, 35 mm.

3.3. Horizontal section analysis of point clouds from laser scanning and from photographs

The next step in assessing the accuracy of shape determination using terrestrial laser scanning data and dense image matching was to assess point cloud cross sections visually. For this purpose, it was decided to select two test fields – a horizontal cross-section at low elevation was made (Fig. 10), including all elements of the object's body with all appendages. The data were superimposed according to the orientation made to a defined coordinate system

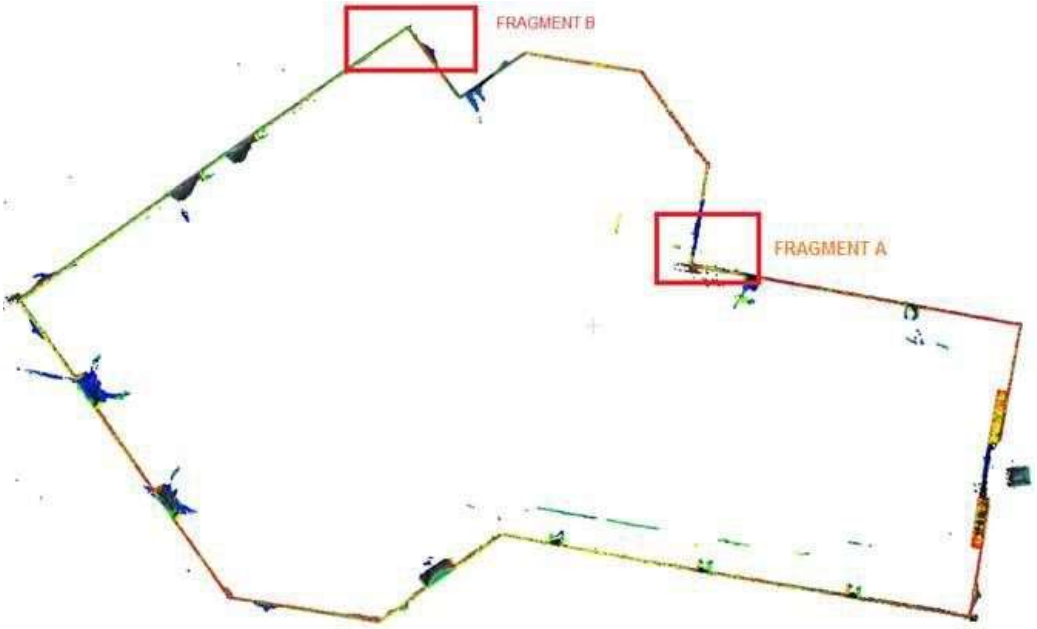

Figure 10. Selected sections of the cross-section

Two representative fragments were selected, containing the corners of the section, both concave and convex. Based on these, the location and nature of each set of points were compared (Fig. 11, 12). Point clouds derived from photographs are marked with red, green and yellow. Those derived from scans in dark brown.

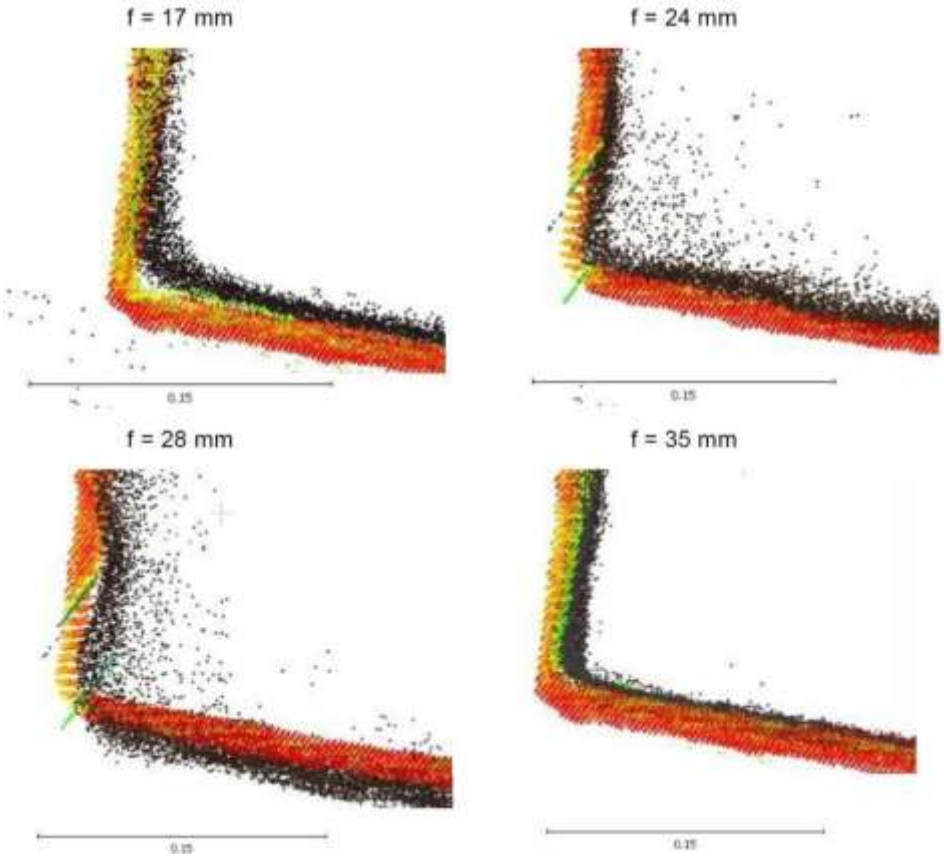

Figure 11. Comparison of section A of the cross-section for each of the point clouds

For fragment A (Fig. 11), the last point cloud was generated from the images taken with a 35mm focal length lens. The point cloud from the photos almost perfectly coincides with the one from the scanning. The object's shape was preserved, there are no outlier points, and deviations of the cloud from the photos from the scanning cloud are at 2 - 3 mm level, exceeding these values minimally for a few groups of points, similarly with the point cloud generated from photos taken with a lens with a focal length of 17 mm. The object's shape was well reproduced, there are no outlier points, and the cloud deviation is about 5 - 8 mm. The worst quality was the point cloud generated from images taken with a lens with a 28 mm focal length. The shape of the object was misrepresented, and the walls are not straight - you can see the "curves" of the building facade in the point cloud from the photos. There are also many points outliers; deviations are even about 5 cm. Also, not very well-mapped point clouds are generated from images taken with a 24 mm focal length lens. There are many outlier points, and the distances between clouds are about 1 - 2 cm.

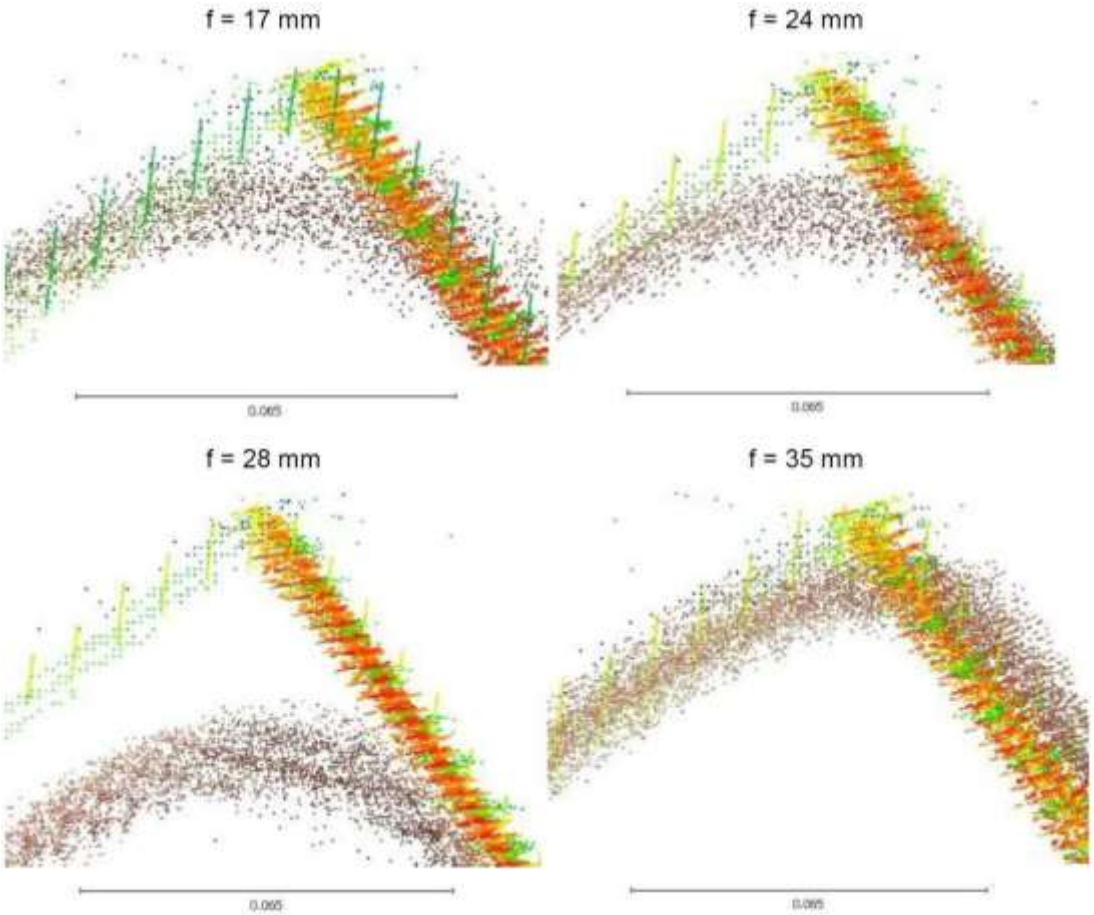

Figure 12. Comparison of section B of the cross section for each of the point clouds

For fragment B (Fig. 12), the analysis results look similar to those for fragment A. The best presentation slice from the last point cloud from a lens with a focal length of 35 mm. The clouds are closest to each other here; the deviation where they do not overlap is about 2 mm. In the case of fragment B, also, not much deviation occurs in the sections for focal lengths of 17 and 24 mm. The sets overlap almost perfectly with each other on the wall fragments; only at the refraction is a cloud deviation visible, amounting to about 2 mm. The largest distances between the point clouds appeared in the slice for images taken with a 28 mm lens. The point clouds on the wall do not overlap, and the distance between them is about 3 mm.

3.4. Vertical section analysis of point clouds from laser scanning and photographs

A vertical section containing the tower was selected for analysis. The excerpted sections came from two opposite sides and were located at different heights (Fig. 13).

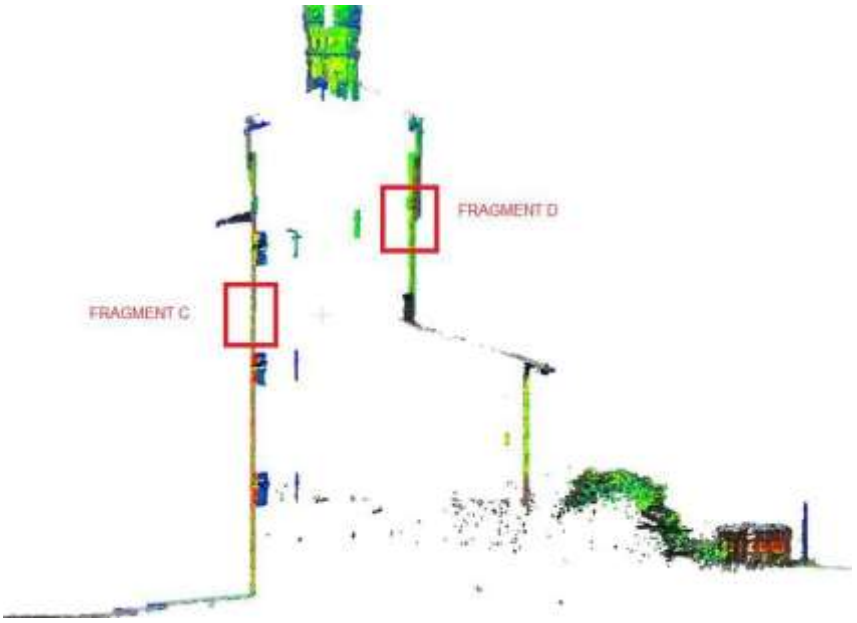

Figure 13. Selected sections of vertical cross-sections

Similarly to the horizontal profile, the study examined the shape and distances of a set of points derived from scanning relative to sets derived from different configurations of images. Figures 14 and 15 also show the scanning data here as darker brown points.

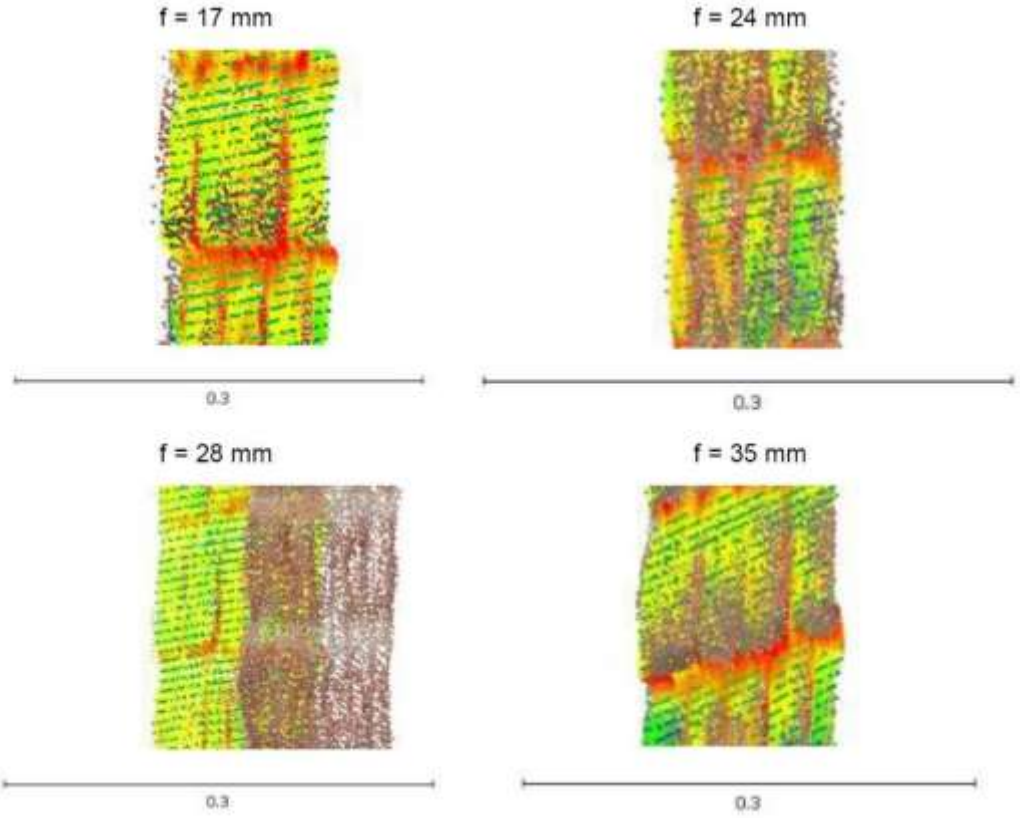

Figure 14. Comparison of section C of the longitudinal section for each of the point clouds

In almost all cases, the object's shape was determined correctly for fragment C (Fig. 14), and the point clouds from the images coincide with those obtained from laser scanning. An offset appears only in the case of data obtained from images with a lens with a focal length of 28 mm. The cloud from the photos is offset from the that obtained from scanning by about 7 cm.

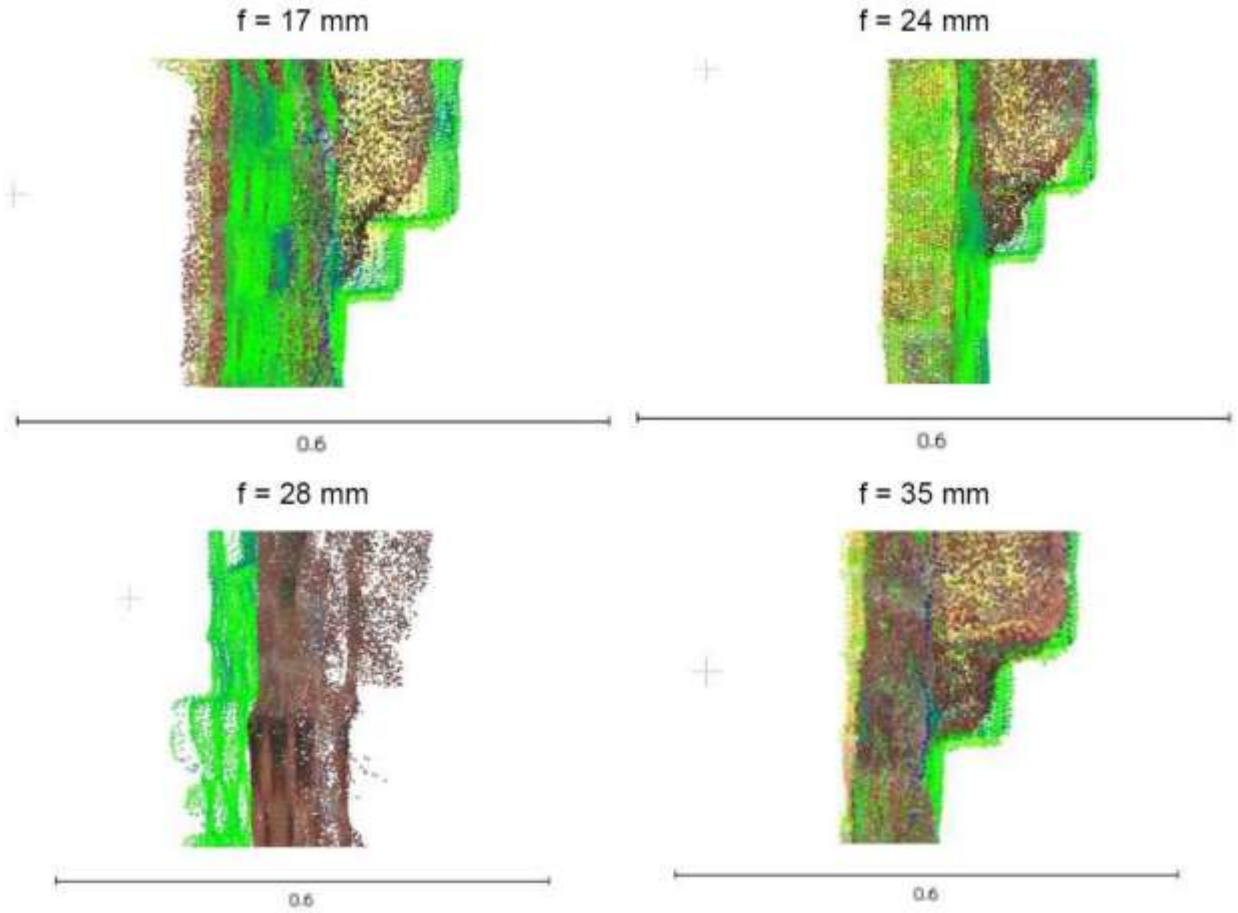

Figure 15. Comparison of section D of the longitudinal section for each of the point clouds

The last slice was measured best for fragment D (Fig. 15). The best results were obtained from the cloud generated from the photos taken with a 35 mm focal length, similar to the one from the scanning, showing characteristic "staircases." In two the first two, the shape is smoothed and less accurate. Again, the worst is the cloud from the images taken with a lens with a focal length of 28 mm. Not only has the shape been misrepresented, but there is also an offset of cloud points amounting to about 7 cm.

3.5. The comparison of the distance between point clouds

The final step of the assessment was to analyse the distance between the point cloud from laser scanning and point clouds extracted from images, using the Cloud2Cloud distance function in CloudCompare software. In this comparison, a slice of the elevation is located from the front of the building (Fig. 16). The reference was a point cloud from laser scanning.

Figure 16. Elevation slice for which distances between point clouds were studied

In Table 2 the result of the distances, histogram of the deviations in meters and the corresponding points numbers are shown.

Table 2. The results of cloud-to-cloud deviations [m] and histograms

f = 17 mm	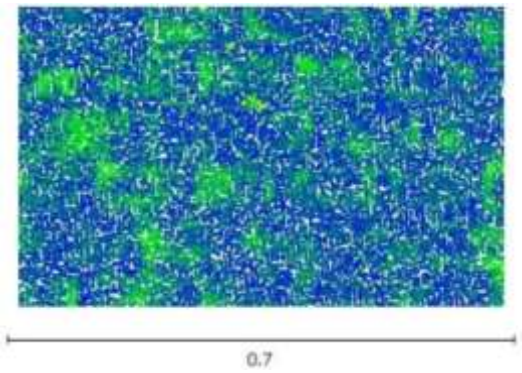	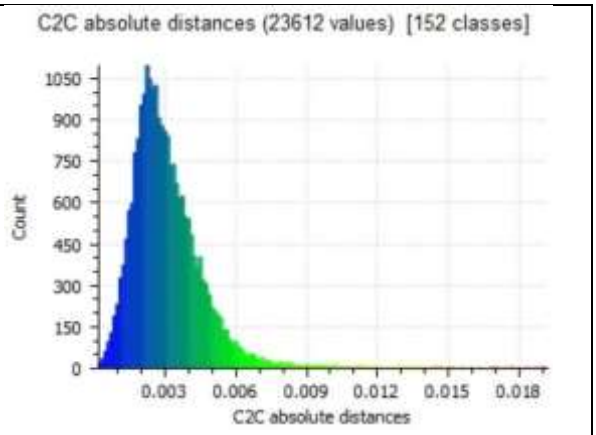
f = 24 mm	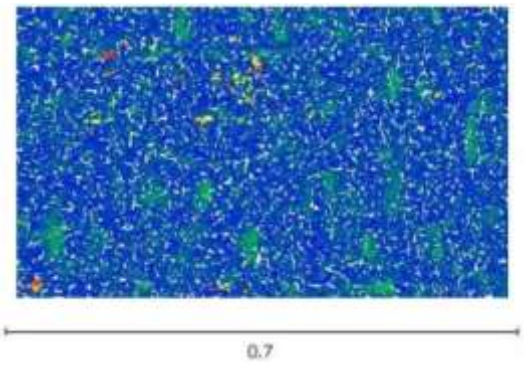	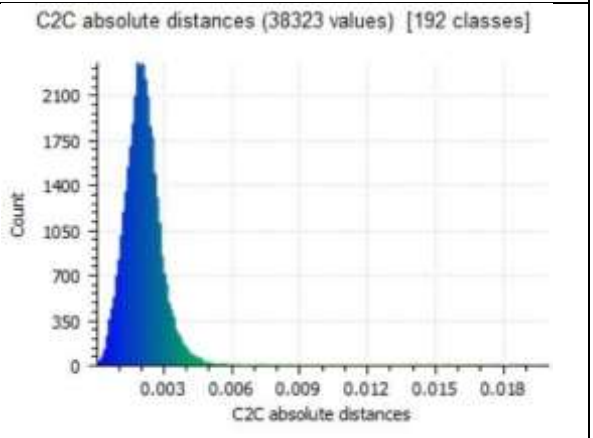

f = 28 mm	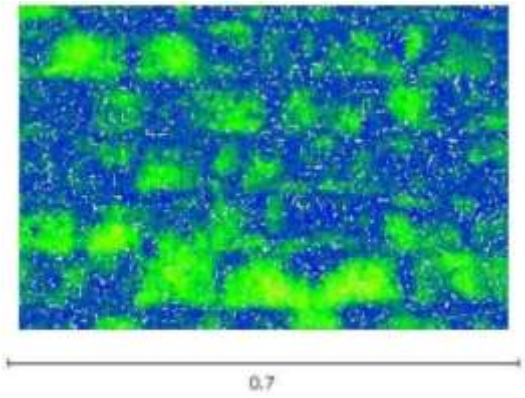	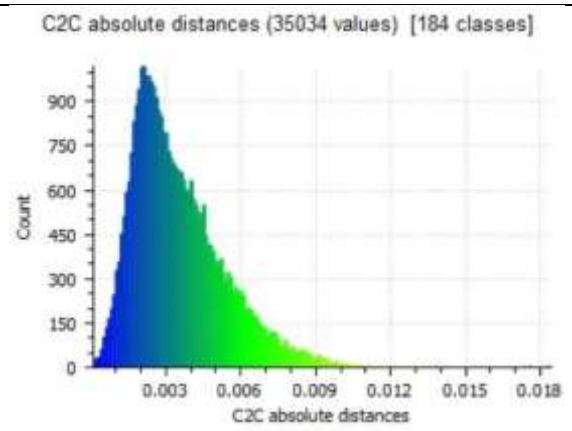
f = 35 mm	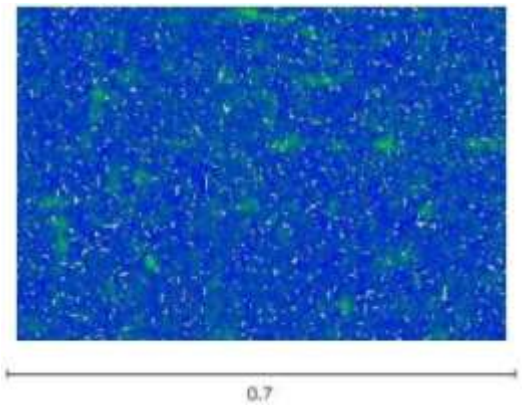	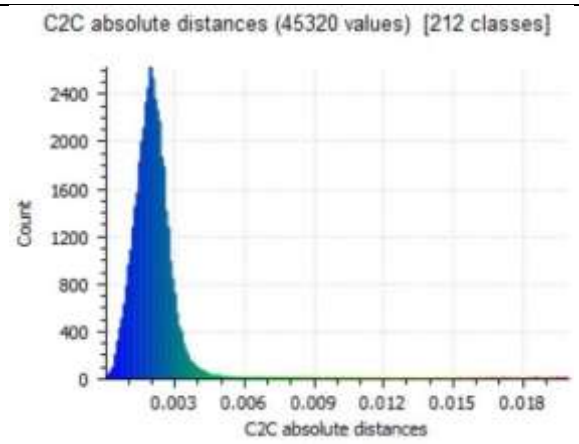

As a result of comparing the distances between point clouds, it was found that for this slice, the highest accuracy is distinguished by the point cloud generated from photos taken with a lens with a focal length of 35 mm. Here the distances between the clouds are about 2 mm. They are higher than 3 mm for a few points and do not exceed 5 mm. Similar accuracy was obtained for the point cloud generated from photos taken with a focal length lens of 24 mm. The lowest accuracy was found for the cloud generated from images taken with a lens with a focal length of 28 mm. The distances relative to the reference cloud reach as high as 9-10 mm for the examined section. The above results are indirectly due to the distances between points. Each set of distances between points in the studied section of point clouds was examined (Table 3).

Table 3. Distances between points in point clouds in the selected slice

Point cloud	Distances between points [mm]
f = 17 mm	4,6
f = 24 mm	4,0
f = 28 mm	4,1
f = 35 mm	3,5
scanning	3,8

3. Discussion and conclusion

Analysing the profiles, one can observe a smoothing of the sharp edges of the object in the case of scanning data (clearly visible in sections B and D). This is caused by the significant width of the radiation beam for a single point, covering a larger portion of the recorded object.

The distributions of deviations between the set of points derived from scanning and those derived from photographs are characteristic of a log-normal description. It occurs when absolute values are examined, unlike the standard normal distribution, which has a symmetrical form.

As a result of comparing the point clouds generated from the images obtained from the four different lenses, the highest accuracy of the last model was found - for the lens with a focal length of 35 mm. Here the distances between the point clouds were the lowest and were about 2 - 3 mm. It is difficult to clearly determine the reason for such a result since all the images were taken on the same day in very similar atmospheric conditions. However, the generation of four point clouds provided an opportunity to compare them and select the most accurate one, i.e. the one closest to the cloud from laser scanning.

In summary, the product in the form of a point cloud generated from digital photos deviates quality from that made by a laser scanner and does not always guarantee satisfactory quality. However, the disadvantage of raw scanning data compared to images is the lack of colour registration. Therefore, combining the two methods is a solution that compensates for their shortcomings. Future work can involve optimising the automatic process of data co-registration, data integration and final documentation generation.

Authors Contributions: J.G., E.K and M.K. organised the conceptualisation of the idea and the methodology employed in this paper. Following that, J.G., E.K and M.K.. carried out the experimental design. J.G. and E.K worked on the data acquisition at the Museum of King Jan III's Palace at Wilanów. M.K. carried out the original writing and draft preparation. J.G., E.K and M.K. undertook the data analysis. All authors have read and agreed to the published version of the manuscript.

Funding: "This research received no external funding".

Conflicts of Interest: "The authors declare no conflict of interest".

References

1. Tobiasz; Markiewicz; Łapiński; Nikel; Kot; Muradov Review of Methods for Documentation, Management, and Sustainability of Cultural Heritage. Case Study: Museum of King Jan III's Palace at Wilanów. *Sustainability* **2019**, *11*, 7046.

2. Stylianidis, E. CIPA - Heritage Documentation: 50 Years: Looking Backwards. *Int. Arch. Photogramm. Remote Sens. Spat. Inf. Sci.* **2019**, *XLII-2/W14*, 1–130.

3. Hatzopoulos, J.N.; Stefanakis, D.; Georgopoulos, A.; Tapinaki, S.; Pantelis, V.; Liritzis, I. Use of various surveying technologies to 3D digital mapping and modelling of cultural heritage structures for maintenance and restoration purposes: The Tholos in Delphi, Greece. *Mediterr. Archaeol. Archaeom.* **2017**, *17*, 311–336.

4. Arif, R.; Essa, K. Evolving Techniques of Documentation of a World Heritage Site in Lahore. *ISPRS - Int. Arch. Photogramm. Remote Sens. Spat. Inf. Sci.* **2017**, *XLII-2/W5*, 33–40.

5. Murtiyoso, A.; Koehl, M.; Grussenmeyer, P.; Freville, T. ACQUISITION and PROCESSING PROTOCOLS for UAV IMAGES: 3D MODELING of HISTORICAL BUILDINGS USING PHOTOGRAMMETRY. In Proceedings of the ISPRS Annals of the Photogrammetry, Remote Sensing and Spatial Information Sciences; 2017; Vol. 4, pp. 163–170.

6. Gonizzi Barsanti, S.; Remondino, F.; Visintini, D. 3D SURVEYING AND

MODELING OF ARCHAEOLOGICAL SITES - SOME CRITICAL ISSUES -. *ISPRS Ann. Photogramm. Remote Sens. Spat. Inf. Sci.* **2013**, *II*, 2–6.

7. Cipriani, L.; Bertacchi, S.; Bertacchi, G. AN OPTIMISED WORKFLOW FOR THE INTERACTIVE EXPERIENCE WITH CULTURAL HERITAGE THROUGH REALITY-BASED 3D MODELS: CASES STUDY IN ARCHAEOLOGICAL AND URBAN COMPLEXES. *ISPRS - Int. Arch. Photogramm. Remote Sens. Spat. Inf. Sci.* **2019**, *XLII-2/W11*, 427–434.

8. Lanteri, L.; Agresti, G.; Pelosi, C. A New Practical Approach for 3D Documentation in Ultraviolet Fluorescence and Infrared Reflectography of Polychromatic Sculptures as Fundamental Step in Restoration. *Heritage* **2019**, *2*, 207–215.

9. Del Pozo, S.; Rodríguez-Gonzálvez, P.; Sánchez-Aparicio, L.J.; Muñoz-Nieto, A.; Hernández-López, D.; Felipe-García, B.; González-Aguilera, D. Multispectral Imaging in Cultural Heritage Conservation. *ISPRS - Int. Arch. Photogramm. Remote Sens. Spat. Inf. Sci.* **2017**, *XLII-2/W5*, 155–162.

10. Clim, D.-A.; Groll, L.; Diaconu, L.-I. Moisture – the Main Cause of the Degradation of Historic Buildings. *Bul. Institutului Politeh. Din Iaşi* **2017**, *63*, 65–78.

11. GIS of Museum of King Jan III's Palace at Wilanów Available online: https://gis.muzeum-wilanow.pl/gis/ (accessed on Dec 9, 2022).

12. Museum of King Jan III's Palace at Wilanów Available online: https://www.wilanow-palac.pl/en (accessed on Dec 9, 2022).

13. Z+F Available online: http://www.zf-laser.com/Home.91.0.html?&L=1 (accessed on Dec 9, 2022).

14. Nyimbili, P.H.; Demirel, H.; Şeker, D.Z.; Erden, T. Structure from Motion (SfM) - Approaches and Applications. In Proceedings of the International Scientific Conference on Applied Sciences, 27-30 September 2016; Antalya, Turkey, 2016.

15. Markiewicz, J.; Pilarska, M.; Łapiński, S.; Kaliszewska, A.; Bieńkowski, R.; Cena, A. Quality assessment of the use of a medium format camera in the investigation of wall paintings: An image-based approach. *Meas. J. Int. Meas. Confed.* **2019**, *132*, 224–237.

16. Shen, S. Accurate multiple view 3D reconstruction using patch-based stereo for large-scale scenes. *IEEE Trans. Image Process.* **2013**, *22*, 1901–1914.

17. Zhang, R.; Schneider, D.; Strauß, B. GENERATION AND COMPARISON OF TLS AND SFM BASED 3D MODELS OF SOLID SHAPES IN HYDROMECHANIC RESEARCH. *Int. Arch. Photogramm. Remote Sens. Spat. Inf. Sci.* **2016**, *XLI-B5*, 925–929.

18. Carraro, F.; Monego, M.; Callegaro, C.; Mazzariol, A.; Perticarini, M.; Menin, A.; Achilli, V.; Bonetto, J.; Giordano, A. THE 3D SURVEY OF THE ROMAN BRIDGE OF SAN LORENZO IN PADOVA (ITALY): A COMPARISON BETWEEN SFM AND TLS METHODOLOGIES APPLIED TO THE ARCH STRUCTURE. *Int. Arch. Photogramm. Remote Sens. Spat. Inf. Sci.* **2019**, *XLII-2/W15*, 255–262.